ELSEVIER

Journal of Nuclear Materials 256 (1998) 25–34

journal of nuclear materials

# The effects of γ-irradiation on subcritical crack growth in alumina

G.P. Pells *, R.M. Boothby

*Nuclear Science, AEA Technology, B. 220, Harwell Laboratory, Didcot, Oxon OX11 0RA, UK*

Received 20 October 1997; accepted 6 March 1998

**Abstract**

A constant load test rig is described which allowed the time to fracture to be measured for ceramic bars loaded in 4-point bending while exposed to 1.5 Gy/s of $^{60}$Co γ-rays. Two grades of alumina, 97.5% and 99.5%, were used to compare subcritical crack growth (SCCG) under constant load with and without exposure to γ-radiation. Dynamic fracture tests on 30 samples of each material were used to determine the Weibull modulus from which the critical failure stress values for the γ-irradiated and non-irradiated samples fractured under constant load could be determined and used to compare failure times. The time to failure for a given ratio of applied stress to critical stress was found to increase by a factor ≈9 for γ-irradiated 97.5% alumina, but the same dose rate reduced the time to failure of the 99.5% alumina by ≈2. Measurement of the length of cracks extending from the tensile surface of test samples showed a much higher proportion of short cracks in a γ-irradiated, 97.5% alumina sample compared to a non-irradiated sample which had predominantly longer cracks. The crack size distribution in γ-irradiated 99.5% alumina showed a significant increase in the number of large cracks leading to a shorter time to failure. It was concluded that ionising radiation inhibits crack growth in aluminas with silica-rich grain boundary phases. 

## 1. Introduction

Studies of radiation effects in ceramics for fusion power plant applications have advanced considerably in recent years and for the technologically important materials such as alumina there exists a reasonable data base on electrical properties, swelling, thermal conductivity and some mechanical properties such as fracture strength. These have been reviewed by Pells [1] for alumina in particular and by Clinard and Hobbs [2], Pells [3] and Dienst [4] for ceramic insulators more generally. However, there is little information on some of the other parameters that would be required for the design of load bearing ceramic components in a fusion power plant. Fett and Munz [5] have recently published data on subcritical crack growth of various grades of alumina of possible use for windows in gyrotron tubes.

Changes in Weibull modulus have been measured after irradiation by Dienst [4] who found that polycrystalline alumina fell from an initial value of ≈9 to 3 after a neutron fluence of $3.7 \times 10^{26}$ n/m$^2$. Silicon carbide showed similar changes but aluminium nitride tended to remain constant although there was a large scatter in the AlN data. Dienst suggested that the post-irradiation fracture results inferred a corresponding reduction in fracture toughness but the only measured data available is that of Clinard et al. [6] who found that, for irradiated sapphire, the fracture toughness increased after a fast neutron fluence of $\approx 1 \times 10^{26}$ n/m$^2$ at 650–825°C. This was thought to be due to crack tip blunting at voids produced by the irradiation.

Most of the existing data on the effects of radiation on mechanical properties of ceramics compares pre-irradiation with post-irradiation values which is probably reasonable for dynamic tests such as fracture strength and fracture toughness where the measured values will be determined largely by the nature of the microstructure existing at the time.

However there have been some in situ measurements of mechanical properties during irradiation using charged particles as the source of radiation damage.

* Corresponding author.

0022-3115/98/$19.00 
PII: S0022-3115(98)00047-6

Zhu and Jung [7] irradiated thin sheets of alumina and silicon carbide with 10.7 MeV protons over the temperature rang 235–505°C under a uniaxial tensile stress ranging from 20 to 100 MPa. The strain rates in both materials showed a sub-linear dose dependence, a slight decrease with increasing temperature and negligible stress dependence. The strain was interpreted as swelling by defect accumulation. Similar measurements with vitreous silica [8] showed that, despite the application of a tensile stress, the samples initially contracted under irradiation which is the normal response of amorphous silica to ionising radiation. With continuing irradiation the strain reversed and the sample began to dilate in the stress direction. The eventual dilation rates showed a linear dependence on dose and stress which was interpreted as viscous flow which, for a constant dose rate of $2.3 \times 10^{-7}$ dpa/s, gave an almost temperature independent viscosity, $\eta$, of $\approx 10^{13}$ Pa s. This is equivalent to the thermal viscosity at ≈1200°C. The viscosity of silica under irradiation decreased linearly with increasing dose rate $K$, i.e. the product $\eta K$ is constant at $\approx 2.3 \times 10^6$ Pa dpa. Similar decreases in viscosity have been reported by Primak [9] using electron irradiation where the irradiating electrons were of too low an energy to produce displacement damage.

The more usual aspects of time dependent mechanical properties such as subcritical crack growth (SCCG) have been largely ignored although Zverev et al. [10] have examined time to fracture of a wide range of electrical insulators in a pulsed neutron field with the samples in air at room temperature. The samples were loaded at stresses within the range 0.5–0.8 of their mean fracture strength and the time to fracture measured while exposed to the pulsed neutron beam. A few measurements were also made under steady state neutron irradiation. It was established that the time to failure under irradiation was inversely proportional to the content of the glass phase in the ceramic.

Fractures in ceramic materials are generally initiated at pre-existing surface microcracks. Using a fracture mechanics approach, failure is predicted to occur when the applied stress intensity $K$ reaches a critical value $K_C$. The applied stress intensity is dependent on the applied stress $\sigma$ and the crack length $a$:

$$K = Y\sigma(a^{1/2}), \tag{1}$$

where $Y$ is a geometrical factor which, in general, is dependent on the shape of the crack and the type of specimen. $K_C$ is a material constant (the 'fracture toughness' value), and hence in dynamic tests a range of failure stresses is exhibited by a ceramic material owing to the naturally occurring distribution of flaw sizes.

For a given flaw size, the dynamic, or instantaneous, failure stress may be denoted by $\sigma_C$. For very brittle materials exhibiting no plasticity, the Griffith fracture criterion

$$K_C = \sigma_C(\pi a)^{1/2} \tag{2}$$

applies. Application of a stress below $\sigma_C$ in a ceramic material will not cause instantaneous failure but may give rise to crack extension at a finite rate – or 'subcritical crack growth'. Only when the crack length reaches the critical length for the applied stress will failure occur. Because there is a distribution of flaw sizes, there will also be a range of failure times for a given applied stress under such static loading conditions. It is conceivable that ionising radiation could influence the rate of subcritical crack growth by affecting the bonding and/or migration of atoms. The present experiment was designed to compare the lifetime of alumina bend-test specimens, loaded at constant stress, under γ-irradiation and non-irradiation conditions.

## 2. Experimental procedure

### 2.1. Sample preparation

Two types of alumina were examined, both being representative of widely used industrial grades. Both grades were supplied by the Morgan Matroc division of the Morgan Crucible, UK. The two materials had the trade names Deranox 975 and Deranox 995, hereafter denoted as D975 and D995. Their specifications are listed in Table 1 from data supplied by Morgan Matroc. Both materials consist of high purity alumina grains with alumino-silicate grain boundaries which were considered to be glassy in the case of D975 and crystalline in D995.

The fracture bars were produced from a number of pressed plates which were then cut into bars and fired under the standard conditions for each grade of material.

Table 1
Composition and mechanical properties

| Alumina grade | Composition (wt%) | | | | Grain size (μm) | Mechanical properties | | |
|---|---|---|---|---|---|---|---|---|
| | $Al_2O_3$ | $SiO_2$ | MgO | CaO | | Fracture strength (MPa) | Weibull modulus | Fracture toughness (MPa $m^{1/2}$) |
| D975 | 97.1 | 1.54 | 0.77 | 0.35 | 2.5–6 | 350 | ≃10 | 3.6 |
| D995 | 99.5 | 0.13 | 0.26 | 0.04 | 8–16 | 330 | ≃10 | 4.0 |

All of the samples of a particular grade were fired in one batch. The bars were then diamond ground to give samples 55 mm long by 4 mm wide by 3 mm deep with a nominal 1 μm finish. The edges of the samples were chamfered at a 45° angle to a width of 0.15 mm.

On receipt of the samples the surface roughness was measured by a Sloan Dectak 2 surface profilometer and it was found that the 97.5% alumina had an average scratch depth of ≈1 μm whereas the 99.5% alumina had an average scratch depth of ≈3 μm with occasional scratches going to 8 μm deep.

### 2.2. Dynamic fracture tests

The samples were tested in 4-point bending for which the applied stress is given by

$$\sigma = (3Px)/bd^2, \tag{3}$$

where $P$ is the applied load, $2x$ the difference between the outer (support) and inner (load point) spans, $b$ the sample width and $d$ the sample depth. In the dynamic tests the inner and outer spans were 20 and 40 mm, respectively. This gives a value for $x$ in Eq. (1) of 10 mm. The tests were made in air at room temperature using a calibrated load cell and a displacement rate of 0.02 mm/min. The fracture strength of 30 samples of each grade of alumina was measured in order to determine the range of critical stress values, $\sigma_C$, for each material.

### 2.3. Constant load tests

A constant load rig was designed that could hold four samples at a time with the samples in close proximity to a $^{60}$Co, γ-ray source at the centre of the rig. A sketch of the rig is given in Fig. 1. The four constant load stations were built around a central steel tube into which the γ-ray source could be inserted. Windows cut in the steel tube allowed the γ-rays unimpeded access to the four samples. The alumina samples were supported in 4-point bending by high speed steel 'knife-edges' having 1 mm radius tips. The spans of the upper and lower loading points were 25 and 50 mm, respectively (i.e. $x = 12.5$ mm). The lower 'knife-edge' blocks were firmly bolted to a steel platform welded to the central support tube and the upper 'knife-edge' blocks were loosely held in position above the samples by four hardened steel guide pins. The load was applied via weights and a 10:1 lever arrangement acting through a ball bearing onto the upper loading block. Two complete rigs were built giving a total of eight test positions.

The nominal load was obtained by multiplying the weight applied at the lever end by ten plus a small contribution ($5N$, determined using a load cell) to allow for the weight of the lever plus load transmission system. There was an estimated uncertainty of ±5% in the total applied load which arose from the difficulty of locating the sample exactly on the load transmission axis.

The load weights were supported by labjacks prior to testing and then the load applied gradually by winding them down. Monitoring of electrical contact between the weights and the labjacks was used to determine the duration of the tests. Breaking the electrical circuit as the weights became completely unsupported, started a PC controlled clock for each individual test and similarly when a sample fractured the falling weight completed the electrical circuit which stopped the clock. Each of the eight available test stations was interrogated by the clock at one second intervals. Failure times ranged from less than a minute to many days. For the tests carried out in the γ-cell there was a delay of ≈5 min between applying the loads and starting the irradiation. To avoid too frequent interruptions of the irradiation and disturbances to the tests in progress, broken samples were generally replaced at 5 day intervals. Samples that remained intact for 10 days or more were removed from the rig. The γ-dose rates were measured at the beginning and end of the tests by red PMMA plastic dosimeters placed in the fracture bar positions and were found to average ≈1.5 Gy/s.

The γ-irradiations for both grades of alumina were split into time blocks with the rigs being removed from the γ-cell for the non-irradiation tests between the two sets of γ-cell tests. Between 30 and 50 samples were used in each group of tests.

## 3. Experimental results

### 3.1. Dynamic 4-point bend tests

The dynamic fracture stress of the D975 alumina samples ranged from 270 to 444 MPa with a mean value of (371.5 ± 41.9) MPa. The critical stress values, $\sigma_C$, were ranked in order from the lowest to the highest to enable a Weibull plot of the failure strengths to be made.

In the Weibull model, a failure probability $F_j$ for the $j$th ranked specimen out of a set of $N$ is defined by

$$(1 - F_j) = 1 - (j/(N + 1)). \tag{4}$$

Provided that the model is applicable, a plot of $-\ln(\ln 1/(1 - F))$ versus $\ln(\sigma_C)$ has a slope of $m$, where $\sigma_C$ is the failure stress and $m$ is the Weibull modulus. The Weibull plot for the D975 set of results where $N = 30$ is given in Fig. 2. A linear regression fit to the data gives

$$\ln(\ln\ 1/(1 - F)) = 9.13\ \ln(\sigma_C) - 54.5. \tag{5}$$

The Weibull modulus of about 9 is fairly typical for a ceramic.

The dynamic fracture stress for the D995 alumina samples had a more narrow distribution ranging from

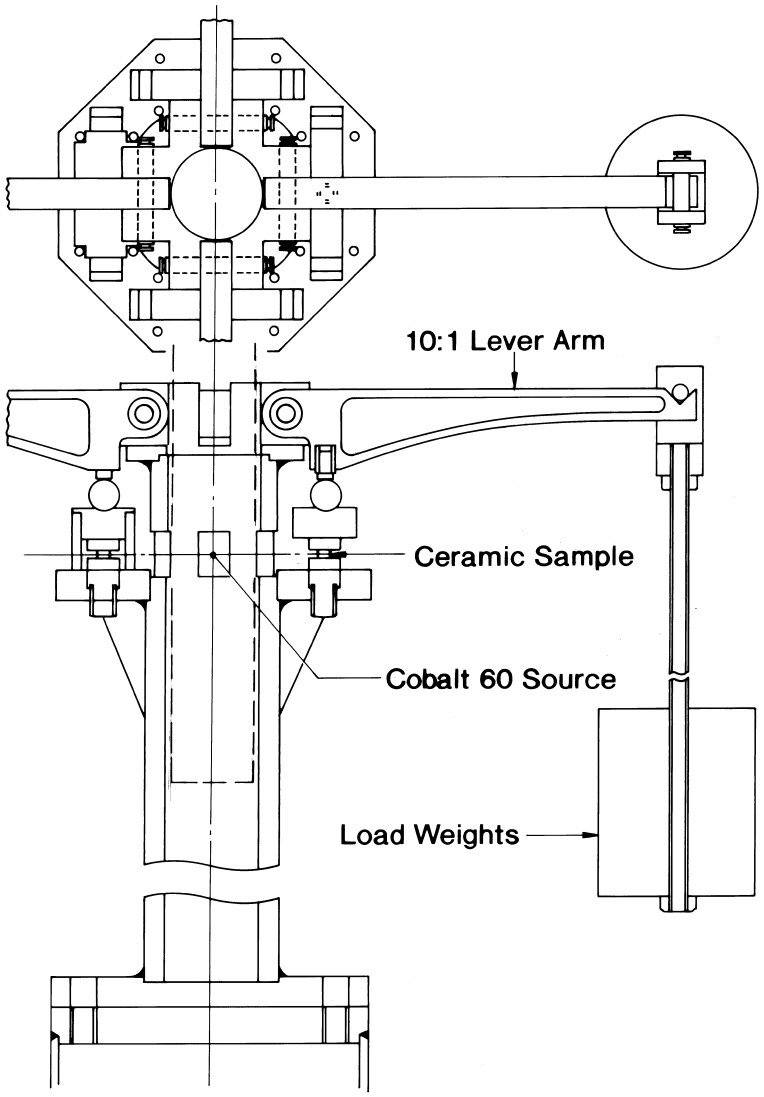


Fig. 1. Schematic diagram of 4-point bend rig for constant load tests.

211 to 271 MPa with a mean of (246 ± 13) MPa. The dynamic fracture test results are collected together in Table 2 and the Weibull plot is given in Fig. 2. The Weibull plots could now be used to estimate $\sigma_C$ values for the $\gamma$-irradiated and unirradiated samples tested under constant load conditions as a basis for comparing the failure times.

### 3.2. Constant load tests

#### 3.2.1. Unirradiated tests

The nominal applied stress, $\sigma_A$, in the D975 constant load tests was 276 MPa, which was marginally above the lowest dynamic failure stress of 270 MPa. The unirradiated set of 32 samples exhibited 20 failures in times ranging from 9 s to 169 h, with 12 samples surviving to 240 h. Fig. 3 shows a plot of the ratio of the applied stress to the critical stress ($\sigma_A/\sigma_C$) as a function of log time to failure. As mentioned above, the values of the critical stress, $\sigma_C$, were derived from the Weibull fit to the dynamic fracture test data by ranking the 20 failures in order and assigning a survival probability value of $(1 - F_j) = (1 - (j/33))$. The predicted dynamic failure stress, $\sigma_C$, was then determined from Eq. (5), enabling a value of ($\sigma_A/\sigma_C$) to be assigned to each sample and plotted against the time to failure.

In the case of the D995 constant load tests the nominal applied stress was 211 MPa which coincided with the lowest dynamic failure stress. The first unirradiated set of 51 samples had 39 failures with times ranging from

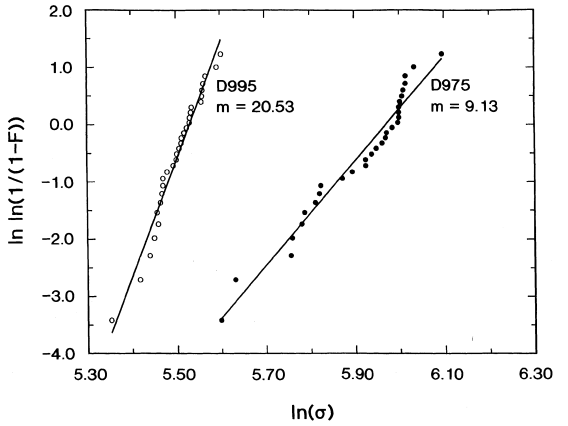


Fig. 2. Weibull plot of dynamic failure stresses for D975 and D995 aluminas.

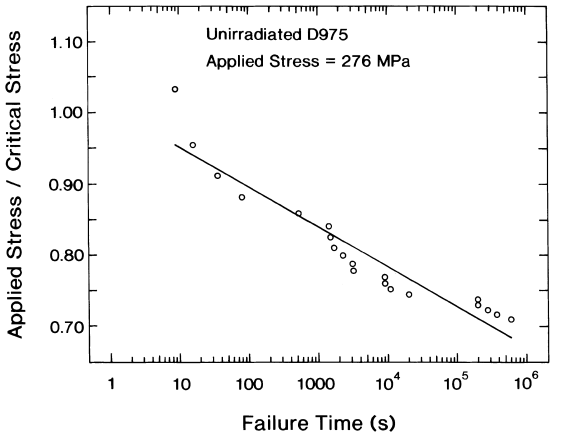


Fig. 3. ($\sigma_A/\sigma_C$) versus log time to failure for unirradiated D975 alumina.

8 s to 180 h. The results are plotted as ($\sigma_A/\sigma_C$) against log time in Fig. 4 with the ratio ($\sigma_A/\sigma_C$) being derived from the Weibull parameters for D995 given in Table 2. The time to fracture of a second set of unirradiated samples was determined after the completion of the γ-irradiation measurements. This set of 23 samples had 18 failures with times ranging from 4 s to 98 h and these results are also given in Fig. 4.

*3.2.2. γ-irradiated tests*

With the rigs transferred to a $^{60}$Co γ-irradiation cell, the static load tests were repeated using the same applied stress (276 MPa for D975 and 211 MPa for D995) as was used for the unirradiated tests. As mentioned previously there was an interval of ≈5 min (300 s) between the application of the static load and the start of the γ-irradiation.

There were 32 samples tested in the first group of D975 of which 16 failed. Three failures occurred before the irradiation had started. The remaining 13 failures occurred in times ranging from 36 min to 124 h. In the second group of irradiations, which occurred 3 months later, 28 samples were tested. Out of these there were two short term failures (unirradiated) and 10 failed during irradiation at times up to 92 h. The two sets of data are presented in Fig. 5 and show some differences between the two. However, the number of data points in each set is low and a greater statistical significance

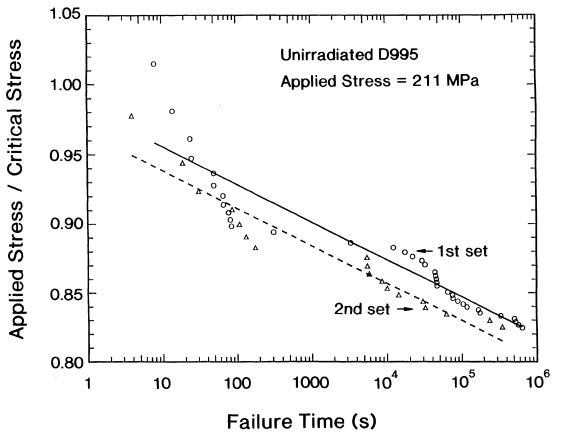


Fig. 4. ($\sigma_A/\sigma_C$) versus log time to failure for 2 sets of unirradiated D995 alumina.

is obtained by combining the two data sets with the result given by the dashed line in Fig. 5.

The combined γ-irradiation data are compared with the unirradiated data in Fig. 6 where it can be seen that γ-irradiation increased the time to fracture under static loading by a factor of 7–11.

The D995 γ-irradiation also occurred in two groups with several months between the sets of measurements. In the first group there were 52 samples tested with 27

Table 2
Results from dynamic fracture tests

| Alumina grade | Range of fracture stress (MPa) | Mean stress ± std. deviation (MPa) | Values derived from Weibull plot | |
|---|---|---|---|---|
| | | | Weibull modulus $m$ | $\sigma_0$ (MPa) |
| D975 | 270–444 | 371 ± 42 | 9.1 | −54.5 |
| D995 | 211–271 | 246 ± 13 | 20.5 | −113.5 |

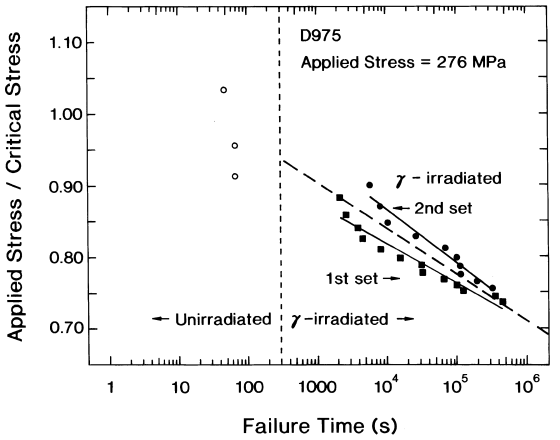


Fig. 5. ($\sigma_A/\sigma_C$) versus log time to failure for two sets of γ-irradiated D975 alumina. The open circles at times <300 s are for samples that fractured before the γ-irradiation started.

fractures occurring during irradiation. The second group had 45 samples tested with 26 fracturing during irradiation. There were 15 and 11 early failures in the two groups in the time between the application of the load and the start of the irradiation. The results for the two sets of tests are given in Fig. 7. When the two data sets are combined there are 53 fractures during irradiation out of a total of 97 tests. The combined result is given in Fig. 8 along with the combined unirradiated test results. In this case it can be seen that γ-irradiation has reduced the time to fracture by a factor of ≈2.

Fett and Munz [11] have shown that, under constant load conditions, the crack velocity ($v$) can be determined from measurements of time to failure ($t_f$) without any knowledge of the $v$–$K_I$ dependence using Eq. (6) given below:

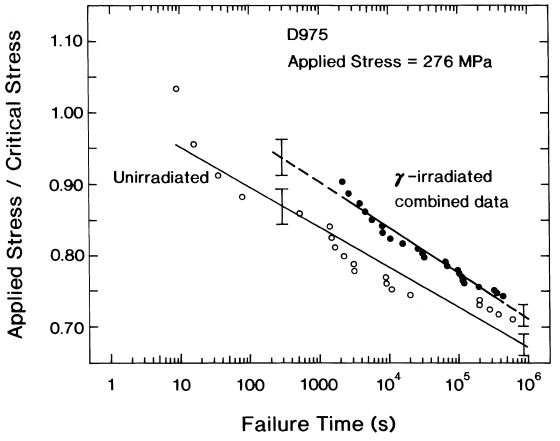


Fig. 6. ($\sigma_A/\sigma_C$) versus log time to failure for unirradiated and γ-irradiated D975 alumina.

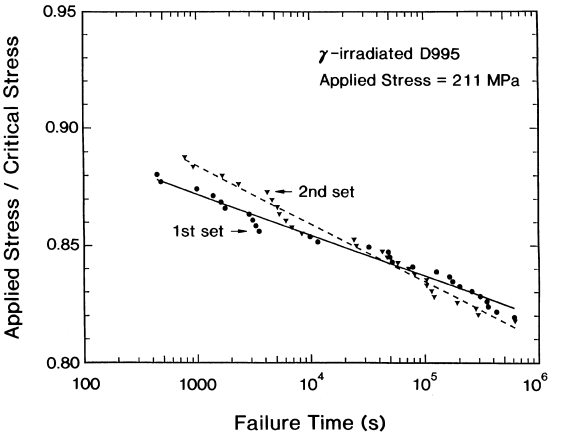


Fig. 7. ($\sigma_A/\sigma_C$) versus log time to failure for the two sets of γ-irradiated D995 alumina.

$$v = \frac{-2K_{IC}^2}{Y^2\sigma_C^2 t_f} \cdot \frac{d[\ln \sigma_A/\sigma_C]}{d[\ln t_f]}. \quad (6)$$

Using the fracture toughness values provided by the sample manufacturers, the crack velocities have been estimated as a function of ($\sigma_A/\sigma_C$) using $Y = \sqrt{\pi}$ and are shown in Figs. 9 and 10 for the two grades of alumina.

### 3.3. Determination of experimental errors

The graphical presentation of ($\sigma_A/\sigma_C$) against log time to fracture for a single data set gives little indication of the errors associated with the measurements because the process of ranking the times to fracture imposes a degree of order on the data which is then scaled in terms of ($\sigma_A/\sigma_C$) by the use of the Weibull constants determined in the dynamic fracture tests. The results presented in Figs. 4, 5 and 7 show that there can be

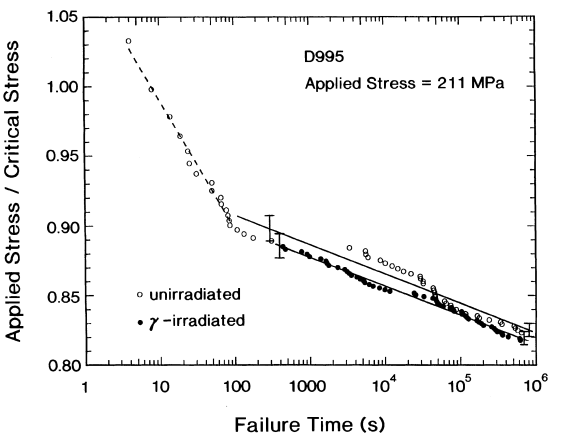


Fig. 8. ($\sigma_A/\sigma_C$) versus log time to failure for unirradiated and γ-irradiated D995 alumina.

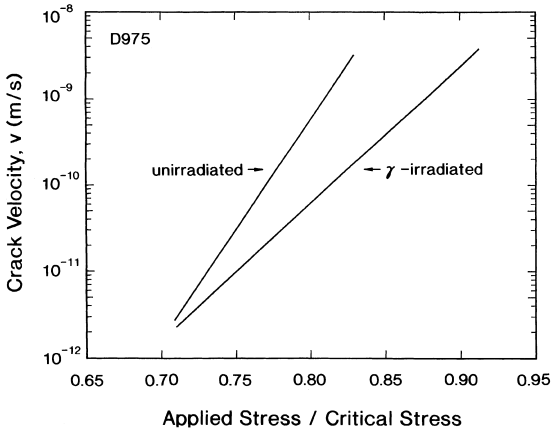


Fig. 9. Calculated crack velocities (Eq. (6)) as a function of the ratio applied stress/critical stress for D975.

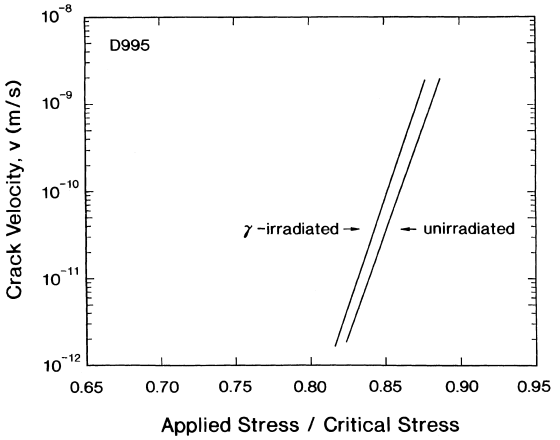


Fig. 10. Calculated crack velocities (Eq. (6)) as a function of the ratio applied stress/critical stress for D995.

considerable differences between data sets containing small numbers of fractures.

The nature and magnitude of the errors involved can be illustrated as follows. A random number generator was used to produce data sets containing 20 times to fracture on a log scale. These times were then converted into graphs of $(\sigma_A/\sigma_C)$: log time using the Weibull parameters determined for D975. The results for five sets are shown in Fig. 11 where it can be seen that the distribution of points and the least squares fit to each data set are qualitatively similar to the real data sets given in Figs. 4, 5 and 7. When the five data sets are combined into one set of 100 points the result is the dashed line in Fig. 11 with error bars representing one standard deviation.

A similar technique was used to determine the errors involved in the actual subcritical crack growth measurements. This involved using all of the experimental data

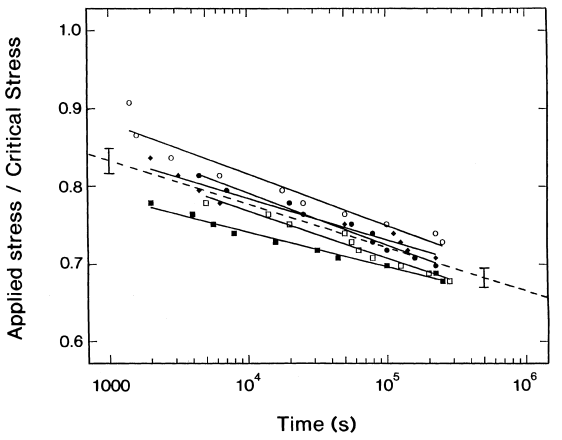


Fig. 11. $(\sigma_A/\sigma_C)$ versus log time to failure plots for five data sets in which a random number generator was used to generate the log time values. The D975 dynamic test data was used to calculate $(\sigma_A/\sigma_C)$. The dashed line results from all of the random times to failure being combined into one data set.

points (both unirradiated and irradiated) for any one material to create a pool of data points from which a number of arbitrary sets, containing the same number of points as the experimental data set under consideration, could be randomly selected with which to determine the statistical scatter about the mean of the randomly chosen sets. The error bars for one standard deviation given in Figs. 6 and 8 were determined in this way.

### 3.4. Microstructural examination

A number of D975 fracture surfaces (three irradiated, three unirradiated and two unirradiated, dynamically fractured) were examined in a scanning electron microscope using a 25 kV electron beam and a range of magnifications ranging from 100× to 1000×. The fracture surfaces showed that the grain size was in agreement with that specified by Morgan Matroc. The fractures seemed to be predominantly intergranular in nature and no differences could be seen between the irradiated and unirradiated samples. Qualitative electron probe micro-analysis examination of polished D975 and D995 cross-sections by Morgan Matroc showed that the grain boundaries in both materials were silicon rich.

A further set of three D975 samples were cross-sectioned to determine the distribution of crack lengths extending from the surface. The three samples included the following:

(1) Part of the stressed centre section of the fracture bar which had exhibited the highest strength in the dynamic fracture tests.

(2) The centre section from an unirradiated, static load, test bar that had survived 10 days without breaking.

(3) The centre section from a static load test bar that had survived 10 days under load in a γ-irradiation field without breaking.

The tensile faces of the two static load samples were glued to the dynamic fracture test bar with epoxy resin held under pressure to give a thin glue line. The glued samples were then diamond ground to remove about 1 mm from the samples followed by polishing down to a 1 μm diamond finish. The polished surfaces were coated with carbon and the samples examined in a Leica S440 SEM working at 30 kV and a magnification of 1500× using a 2.5 μA probe size at a working distance of 14 mm.

The close proximity of the glued faces had provided good mutual support for adjacent samples so that edge retention was excellent with negligible rounding or cracking at the edges. The samples were scanned along joint lines and the microstructure recorded at 25 positions along the 10 mm long edges. The pictures were taken in the backscattered electron mode and a typical area showing medium length cracks is given in Fig. 12. The photomicrographs were subsequently examined for evidence of cracking and the number and lengths of cracks extending from the surface were recorded. The results are given in the histogram (Fig. 13) which shows the frequency with which cracks occurred as a function of crack length normal to the surface. The total number of cracks found for each sample were similar, ranging from 166 for the unirradiated, static load sample to 176 for the dynamic test sample, but the distribution of crack sizes was very different. The dynamic fracture test bar had a maximum number of short cracks of length 5–10 μm although some cracks extended to about 60 μm. The γ-irradiated, constant load sample had a similar distribution but with a larger number of small (<5 μm) cracks at the surface and no cracks greater than 40 μm long. 91% of the cracks were <20 μm long compared with 83% for the dynamic test bar. The unirradiated static load sample had a much more uniform distribution of crack lengths with only a few cracks of <5 μm length and ≈40% of the total number of cracks being >20 μm long including some of >60 μm length.

In all cases the majority of the cracks were intergranular in nature but some transgranular cracking was evident in the longer cracks of the unirradiated sample whereas only a few transgranular cracks were found in the γ-irradiated sample.

## 4. Discussion

In this first quantitative study of the effects of ionising radiation on subcritical crack growth in a refractory ceramic such as alumina, it has been clearly shown that ionisation does effect the rate at which cracks grow under constant load. In the case of the 97.5% alumina the crack velocity was reduced by radiation and in the case of the 99.5% alumina it was increased. At the

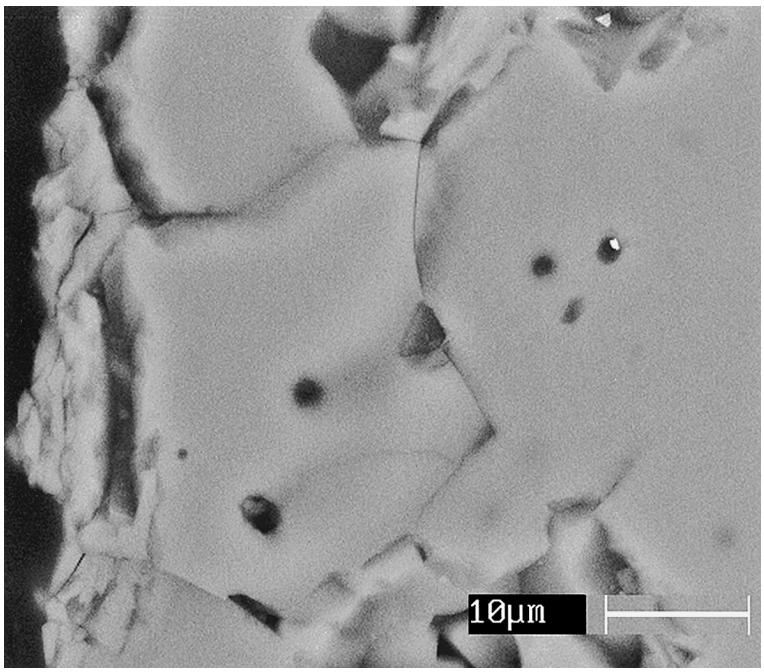


Fig. 12. Back scattered electron SEM image of fractures at the tensile surface of an unirradiated D975 sample that had survived 10 days under a load of 276 MPa without failure.

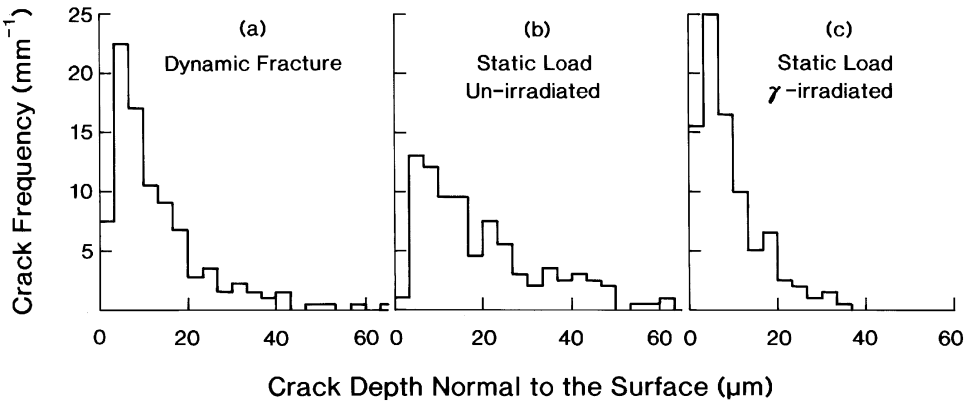


Fig. 13. Histograms of the number of cracks as a function of crack length normal to the surface for D975 fracture bars: (a) after dynamic loading to fracture; (b) after 10 days under a static load of 276 MPa; (c) after 10 days exposed to γ-irradiation and a static load of 276 MPa.

relatively low γ-dose rates used (1.5 Gy/s compared with ≈1000 Gy/s in a fusion power plant) the effects were surprisingly large, with the time to fracture for D975 alumina increasing by a factor of about 9 when exposed to γ-irradiation and that of D995 alumina decreasing by a factor of about 2. The statistical differences in the time to failure of D975 exposed to γ-irradiation compared with that of the unirradiated material was clearly confirmed by the variation in crack size distributions found in the microstructure of the polished cross-sections.

The distribution of crack sizes shown in Fig. 13 for unirradiated and γ-irradiated samples under static load are clearly different with 40% of the cracks in the unirradiated sample being >20 μm deep compared with only 9% of the cracks in the γ-irradiated sample. None of the latter exceeded 40 μm in length whereas 11% of the unirradiated sample cracks exceeded 40 μm with a few exceeding 60 μm. At the other end of the scale, the γ-irradiated sample had 18% of cracks of <3 μm depth compared with about 1% of cracks in the unirradiated sample. These differences indicate that surface cracks in the unirradiated sample were free to grow under a high static load and a few cracks were of a similar order to the calculated critical crack length for D975 alumina under a static load of 276 MPa of 54 μm. However, in the case of the γ-irradiated sample none of the observed cracks exceeded 35 μm in length and there was a high proportion of short cracks at the surface which indicates that γ-irradiation inhibits crack growth in this grade of alumina.

The great majority of cracks, in all of the cross-sections examined, were intergranular although the unirradiated sample showed some mixed inter- and transgranular cracking, particularly in the longer cracks. Therefore it would seem that ionising radiation predominantly effects the high silica, grain boundary phase of the D975 alumina. The lower grain boundary silica content in D995 would seem to result in an increase in SCCG rate.

The mechanism by which ionising radiation changes subcritical crack velocities is not clear at this stage although a few simple statements can be made about the nature and number of defects produced by ionisation.

### 4.1. Defect creation and mobility

Ionisation events in the locality of the crack tip might effect the crack growth rate directly. The probability of this can be calculated. The experimental dose rate was 1.5 Gy/s which is equivalent to $9.9 \times 10^{15}$eV/g s therefore, with a silica band gap is ≈9.5 eV, the number of ions excited in 1g of material in 1s will be about $10^{15}$. The probability of an atom in the locality of the crack tip being ionised is $\approx 10^{-7}$/s which is insufficient to influence the crack tip growth rate. However, such an ionisation rate might be sufficient to effect the bulk diffusion rate for defects.

The crack tip propagation rate depends primarily on the flow of defects to the crack tip. A theoretical study of the stress driven migration of point defects to a crack has been made by Rauh and Bullough [12] who found that when the relaxation volume, $\Delta V$, of a point defect is greater than nought then the defects diffuse to the crack tip and when $\Delta V < 0$ the point defects flow only into the crack surfaces behind the crack tip. Point defects with relaxation volumes of different signs follow the same trajectories in opposite directions with the consequence that, for a fixed magnitude of parameters involved, the numbers of point defects at either the crack tip or the crack faces agree exactly. In general, interstitials (with $\Delta V > 0$) should flow to the crack tip whereas vacancies (with $\Delta V < 0$) should flow to the surfaces behind the actual tip. In the absence of radiation the effects are transitory as the intrinsic defects are used

up. In the case of irradiation with the constant production of point defects the effects are steady state.

Displacement damage in silica occurs on the oxygen sublattice alone and for $^{60}$Co $\gamma$-rays is variously estimated to give $10^6$–$10^7$ defects/cm$^3$/Gy [13,14]. In the present work this equates to $10^{-12}$–$10^{-11}$ dpa/s or a few microdpa per day (dpa = displacements per atom). The question is then, is this defect production rate sufficient to alter the rate of crack tip growth?

The crack tip length required to produce failure in these tests can be calculated from the Griffith criterion for linear elastic fracture given in Eq. (2). For D975, $K_{IC} = 3.6$ MPa m$^{1/2}$ and $\sigma$ in 4-point bend tests was 265 MPa which gives a crack length of 54 μm. If the time to fracture in the tests was 5 days, then the rate at which atoms would have to flow to or from an atom plane normal to the crack tip to propagate that crack would be about 1 per second. The normal diffusion coefficient of oxygen in silica is $\approx 6 \times 10^{-24}$ cm$^2$/s, therefore if oxygen interstitial/vacancy pairs are only being produced at a rate of $\approx 10^{-11}$/s these clearly are not capable of influencing the crack tip growth rate. However, silicate glasses are amorphous because of the large fraction of broken bonds within the structure (approximately 10% of the bonds are broken) and the broken bonds may be regarded as defects. Ionising radiation has been shown to reduce the activation energy for motion of existing defects by a significant amount. Although experimental data is not available for silica the evidence from other insulating materials suggests that the activation energy for motion could be reduced from its normal value of ≈1.2–0.5 eV. This would be sufficient to provide a defect flow of the correct order of magnitude to effect crack tip growth rates.

One ionisation phenomenon that might be capable of producing sufficient 'defects' involves the hydrogen that is always present in oxides, usually as the $OH^-$ molecule. Ionising radiation breaks up the hydroxyl molecule to give either hydrogen atoms or hydrogen molecules. The activation energy for diffusion of the hydrogen atom is only 0.18 eV [15] with a diffusion coefficient at room temperature of $9.5 \times 10^{-8}$ cm$^2$/s. This means that any hydrogen atom within a radius of $\simeq 5$ μm could diffuse into a crack tip within a 1s time interval. There is typically 0.1% of hydrogen in oxide ceramics, making about $10^6$ hydrogen atoms available per second. It is not clear whether $\Delta V$ for hydrogen in the Rauh and Bullough formalism would be positive or negative and so be driven by the stress field to accumulate at the crack tip or crack sides.

## 5. Conclusions

A quantitative study of the effects of ionising radiation on subcritical crack growth in two grades of alumina has shown that the time to fracture of 97.5% alumina under constant load and exposure to 1.5 Gy/s of $\gamma$-radiation increased by a factor of about 9 when compared with the time to fracture without irradiation, whereas that for a 99.5% alumina decreased by a factor of about 2.

Examination of the microstructure of the 97.5% alumina showed that $\gamma$-irradiation inhibited crack growth under load thereby giving longer times to failure. The effects of radiation on SCCG are probably determined by the detailed microstructure of the alumina grain boundary phases.

## Acknowledgements

This work was part of the programme of the UKAEA/Euratom Fusion Association. It was funded by the UK Department of Trade and Industry and Euratom. The authors are indebted to Mr B.C. Sowden for his help in setting up the static load rigs in the $\gamma$-irradiation cells and for the computer programme used to monitor the constant load stations and record the time to failure of the samples. Thanks are also due to Mr S.J. Andrews for performing the dynamic fracture measurements.

## References

[1] G.P. Pells, J. Am. Ceram. Soc. 77 (1994) 368.
[2] F.W. Clinard, L.W. Hobbs, in: R.A. Johnson, A.N. Orlow (Eds.), Physics of Radiation Effects in Crystals, Elsevier, Amsterdam, 1986, p. 387.
[3] G.P. Pells, in: I.M. Robertson, L.E. Rehn, S.J. Zinkle, W.J. Phythian (Eds.), Microstructure of Irradiated Materials, MRS Symposium Proceedings, vol. 373, 1995, p. 273.
[4] W. Dienst, J. Nucl. Mater. 211 (1994) 186.
[5] T. Fett, D. Munz, Fusion Technol. 32 (1997) 170.
[6] F.W. Clinard, G.F. Hurley, R.A. Youngman, L.W. Hobbs, J. Nucl. Mater. 133&134 (1985) 701.
[7] Z. Zhu, P. Jung, J. Nucl. Mater. 212–215 (1994) 1081.
[8] Z. Zhu, P. Jung, Nucl. Instrum. Meth. B 91 (1994) 269.
[9] W. Primak, J. Appl. Phys. 53 (1982) 7331.
[10] Y.B. Zverov, V.I. Ponomarev, N.S. Kostyukov, Y.F. Tuturov, Sov. J. At. En. 49 (1980) 625.
[11] T. Fett, D. Munz, J. Am. Ceram. Soc. 68 (1985) C–213.
[12] H. Rauh, R. Bullough, Proc. R. Soc. London A 397 (1985) 121.
[13] R.A.B. Devine, Phys. Rev. B 35 (1987) 9783.
[14] D.L. Griscom, in: Proceedings of Radiation Effects in Optical Materials, SPIE (Society of Photo-optical Instrumentation Engineers), Albuquerque, New Mexico, 6 and 7 March (1985), vol. 541, p. 38.
[15] D.L. Griscom, J. Appl. Phys. 58 (1985) 2524.